Supporting Information

Two porous-layered borates built by $B_7O_{13}(OH)$ clusters and AlO_4/GaO_4 tetrahedra

Ya-Zhuo Dong,[a] Chong-An Chen,[a] Juan Chen,[a] Jian-Wen Cheng[b] Jin-Hua Li,*[c] and Guo-Yu Yang*[a]*

[a]*MOE Key Laboratory of Cluster Science, School of Chemistry and Chemical Engineering, Beijing Institute of Technology, Beijing 100081, China. *E-mail: ygy@bit.edu.cn.*

[b]*Key Laboratory of the Ministry of Education for Advanced Catalysis Materials, Institute of Physical Chemistry, Zhejiang Normal University, Jinhua, Zhejiang 321004, China. *E-mail: jwcheng@zjnu.cn.*

[c] *School of Chemistry and Chemical Engineering*, *Qingdao University, Qingdao, Shandong 266071, China. *E-mail: jinhuali1978@163.com.*

Figure S1. The experimental and simulated PXRD patterns of **1-2**.

Figure S2. Two types of 8-R windows in **1** along the *a*-axis.

Figure S3. 8-R windows in **1** along the *c*-axis.

Figure S4. (a)View of the 3-D B-O framework along the *b*-axis; (b) View of the 2-D alkali metal-oxygen layers; (c) View of the whole structure of **1**.

Figure S5. Two types of 8-R windows in **2** along the *b*-axis.

Figure S6. (a) View of the 3-D B-O framework along the *b*-axis; (b) View of the 3-D alkali metal-oxygen network; (c) View of the whole structure of **2**.

Figure S7. View of eight types of channels A, B, C, D, E, F, G, and H of **1**, showing channels A, B, C and F only built by one type of the window, and channels D, E, G, and H made of two types of windows, respectively.

Figure S8. View of eight types of channels A, B, C, D, and E of **1**, showing channels A/B only built by one type of the window, and channels C/D/E made of four/three/two types of windows, respectively.

Figure S9. View of the intercommunicated channel systems in $Ba[MB_4O_8(OH)]\cdot H_2O$ (M=Al, Ga) (a); $Ba_3M_2[B_3O_6(OH)]_2[B_4O_7(OH)_2]$ (M=Al/Ga) (b); $[H_3O]K_{3.52}Na_{3.48}\{Al_2[B_7O_{13}(OH)][B_5O_{10}]$-$[B_3O_5]\}[CO_3]$ (c)

Figure S10. IR spectra of **1-2**.

Figure S11. TG curves of **1-2**.

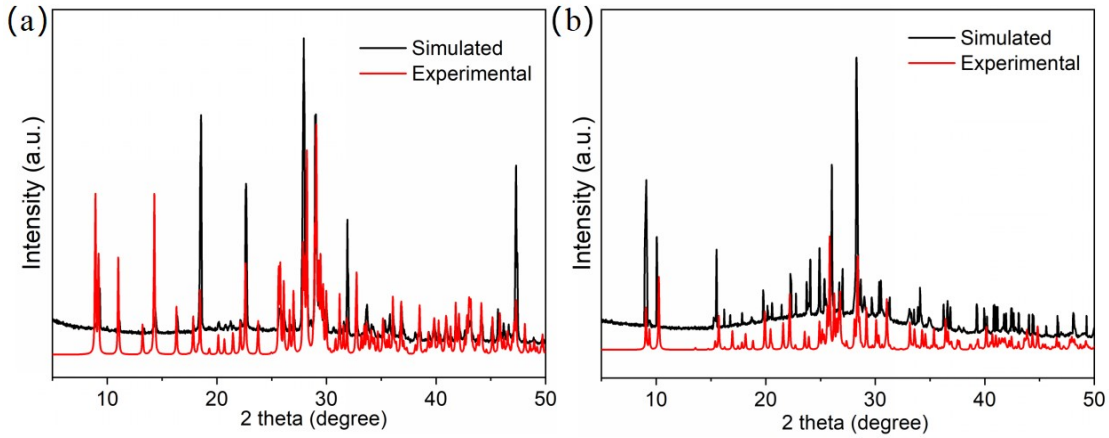

Figure S1. The experimental and simulated PXRD patterns of **1-2**.

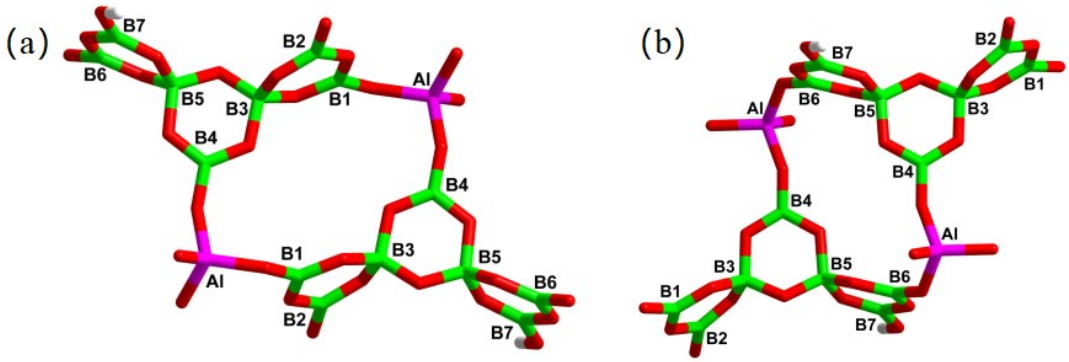

Figure S2. Two types of 8-R windows in **1** along the *a*-axis.

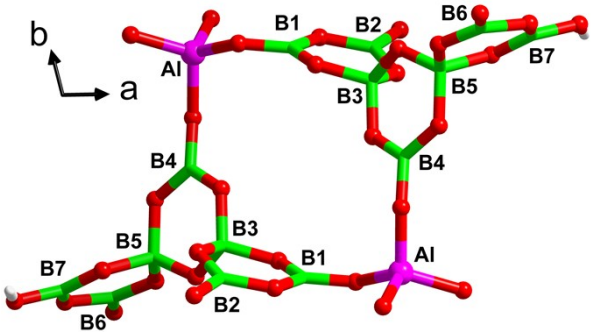

Figure S3. 8-R windows in **1** along the *c*-axis.

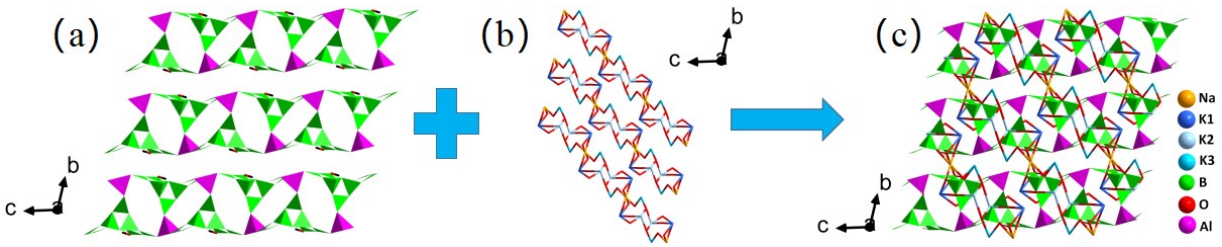

Figure S4. (a)View of the 3-D B-O framework along the *b*-axis; (b) View of the 2-D alkali metal-oxygen layers; (c) View of the whole structure of **1**.

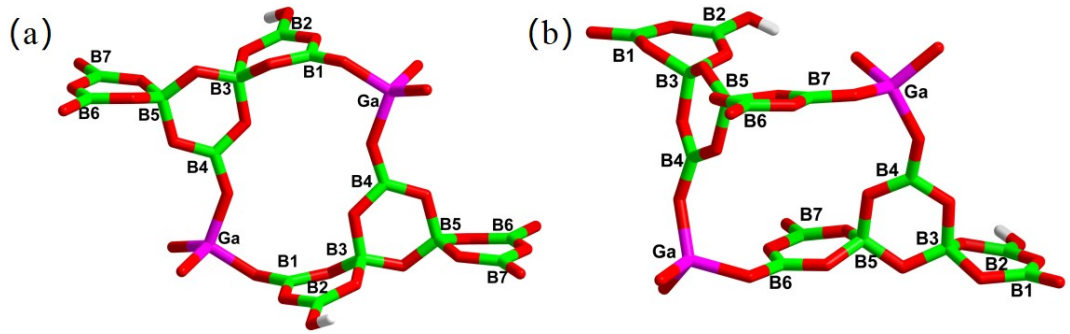

Figure S5. Two types of 8-R windows in **2** along the *b*-axis.

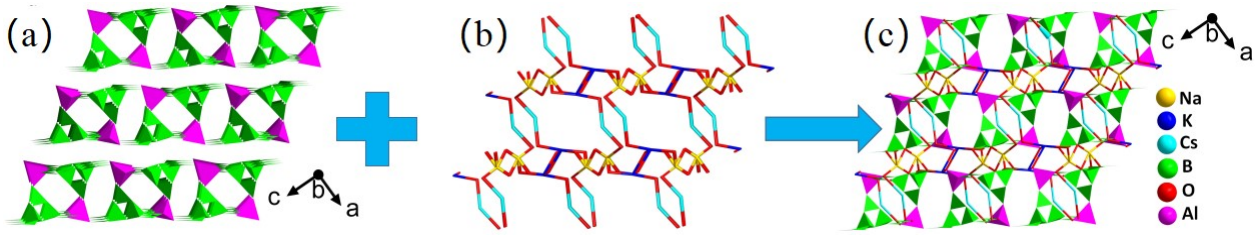

Figure S6. (a)View of the 3-D B-O framework along the *b*-axis; (b) View of the 3-D alkali metal-oxygen network; (c) View of the whole structure of **2**.

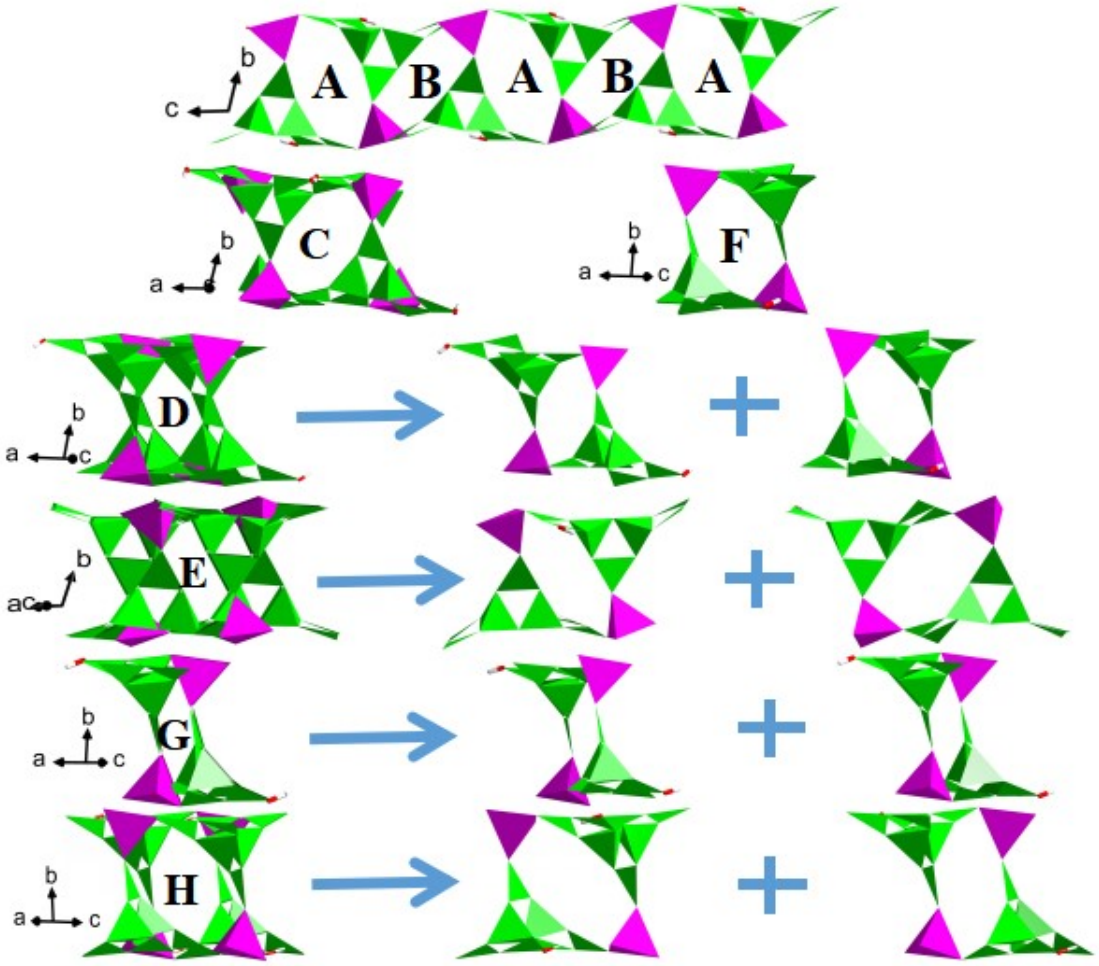

Figure S7. View of eight types of channels A, B, C, D, E, F, G, and H of **1**, showing channels A, B, C and F only built by one type of the window, and channels D, E, G, and H made of two types of windows, respectively.

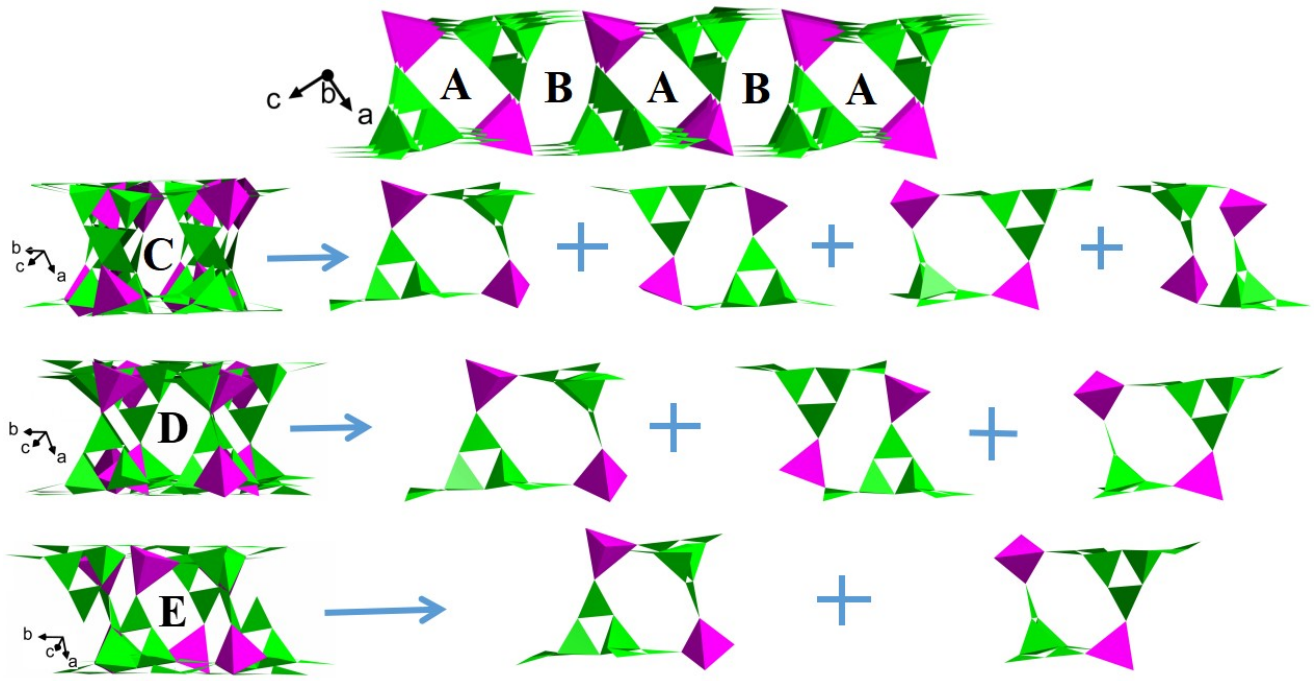

Figure S8. View of eight types of channels A, B, C, D, and E of **1**, showing channels A/B only built by one type of the window, and channels C/D/E made of four/three/two types of windows, respectively.

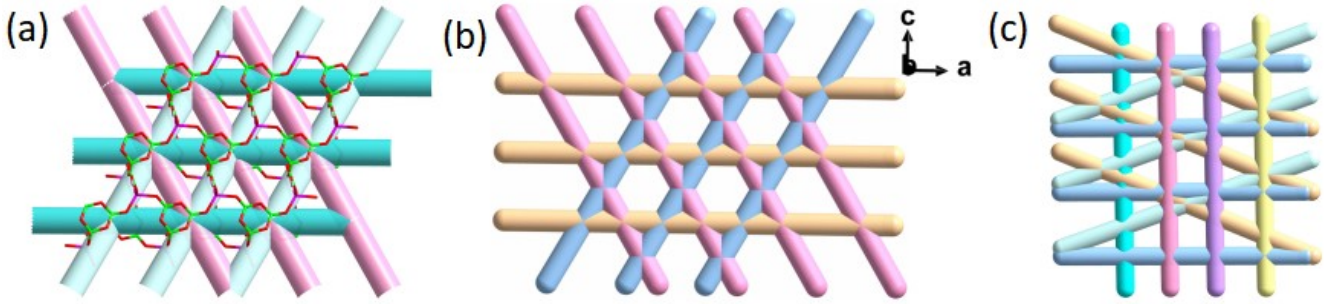

Figure S9. View of the intercommunicated channel systems in $Ba[MB_4O_8(OH)]\cdot H_2O$ (M=Al/Ga) (a); $Ba_3M_2[B_3O_6(OH)]_2$-$[B_4O_7(OH)_2]$ (M=Al/Ga) (b); $[H_3O]K_{3.52}Na_{3.48}\{Al_2[B_7O_{13}(OH)][B_5O_{10}][B_3O_5]\}[CO_3]$ (c), respectively.

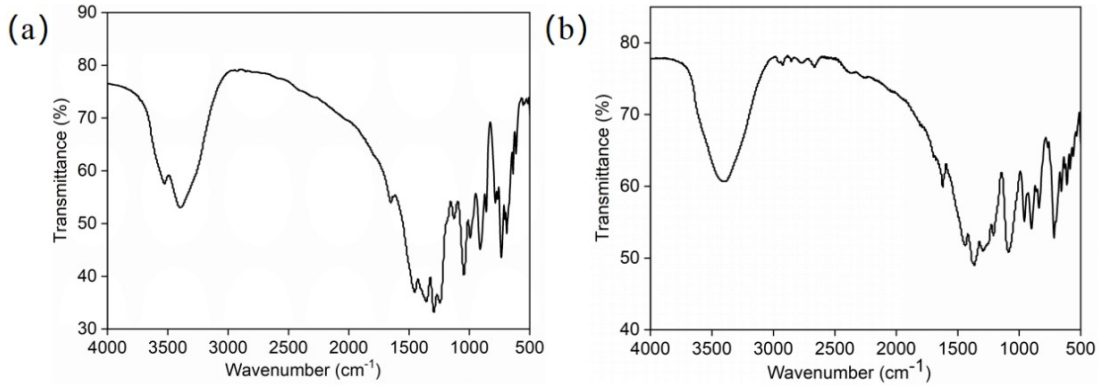

Figure S10. IR spectra of **1**-**2**.

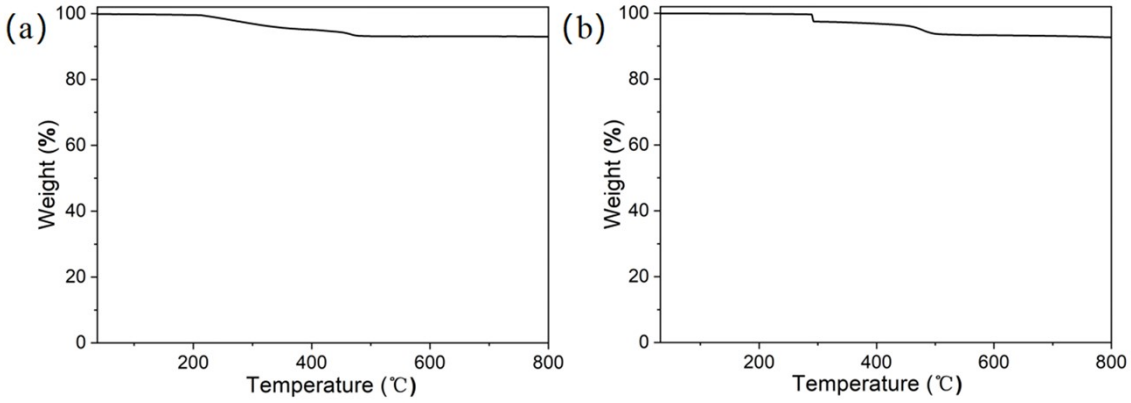

Figure S11. TG curves of **1**-**2**.